Journal of Instrumentation

SISSA

Development of a Triple-GEM detector with strip readout and GEMINI chip for X rays and neutron imaging

To cite this article: F. Caruggi *et al* 2024 *JINST* **19** C02015

Published by IOP Publishing for Sissa Medialab

Received: *October 25, 2023*
Accepted: *December 11, 2023*
Published: *February 2, 2024*

International Workshop on Imaging
Varenna (Lake Como), Italy
26–29 September 2023

Development of a Triple-GEM detector with strip readout and GEMINI chip for X rays and neutron imaging

F. Caruggi, [a,b,*] **A. Celora**, [a] **S. Cancelli**, [a,b] **G. Gorini**, [a,b,c] **G. Grosso**, [c] **F. Guiotto**, [d] **A. Muraro**, [c] **E. Perelli Cippo**, [c] **M. Petruzzo**, [a] **O. Putignano**, [c] **M. Tardocchi**, [b,c] **L.S. Giarratana**[e] **and G. Croci**[a,b,c]

[a] *Dipartimento di Fisica "G. Occhialini", University of Milano-Bicocca, Piazza della Scienza 3, Milano, Italy*
[b] *INFN Sezione Milano-Bicocca, Piazza della Scienza 3, Milano, Italy*
[c] *Istituto per la Scienza e Tecnologia dei Plasmi, CNR, via Cozzi 53, Milano, Italy*
[d] *Dipartimento di Fisica, Università di Padova, via F. Marzolo 8, Padova, Italy*
[e] *Ospedale dei Bambini "Vittore Buzzi", ASST Fatebenefratelli Sacco, via Castelvetro 32, Milano, Italy*

E-mail: `f.caruggi@campus.unimib.it`

Abstract: Thermal neutron imaging can be a useful tool in the study of the internal structure of an object. The different attenuation properties of the materials with respect to X rays give rise to different interactions and the result is a complementary non-destructive analysis, which can provide important additional information. This technique has been successfully employed in different areas of work, especially in material science and cultural heritage studies. This paper describes the development of a new detection system and its characterization performed with X ray emissions. The system features the use of a gaseous detector, based on the Gas Electron Multiplier technology, and a fully digital electronic readout, with a combination of custom-made ASICs (called GEMINI) and FPGA boards, enabling fast single photon counting. The detector can be thus used directly for X ray imaging, while the addition of a suitable converter in its active volume will allow for detection of neutrons and for reconstruction of their tracks. The readout system is based on a x-y strip structure and features the reconstruction of single events through the center of mass methodology, allowing for accurate tomography, with sub-mm spatial resolution, in combination with sub-ms time resolution and high rate capabilities (up to MHz/mm^2).

Keywords: Inspection with neutrons; Inspection with x-rays; Micropattern gaseous detectors (MSGC, GEM, THGEM, RETHGEM, MHSP, MICROPIC, MICROMEGAS, InGrid, etc); CMOS readout of gaseous detectors

---

[*] Corresponding author.

https://doi.org/10.1088/1748-0221/19/02/C02015

2024 JINST 19 C02015

2024 JINST 19 C02015

Contents

1 Introduction

Imaging techniques have become widespread and much useful in various fields of study, allowing for non-destructive investigation of different samples, especially in material science [1] and cultural heritage [2, 3] studies. In this context, both X-rays and neutrons are employed, giving complementary information about the observed objects. The research for faster and more accurate radiation detectors, together with the development of new and better data analysis software and reconstruction techniques are needed for the betterment of imaging studies. In this framework, detectors based on the Gas Electron Multiplier (GEM) principle can be employed, both for X-rays and neutrons (exploiting suitable converters). This kind of detectors features great temporal resolution, high-rate capabilities and radiation hardness, combined with good spatial and energy resolution altogether. In the following, the description of the system and its working principle will first be presented, to then describe the characterization, as well as preliminary results of X ray imaging on different samples. Perspectives for the upgrade of the system for neutron detection will be presented as well.

2 STRIP-GEM detector

The gaseous detector developed in this work is based on the interaction of incoming X-rays with a mixture of Ar-CO2 (70–30%) in the active volume, with ionization and production of electrons. Gas Electron Multiplier (GEM) foils are sheets of kapton, 50 μm thick, metal-coated on both sides (5 μm layer of Copper), with a high-density pattern of biconical holes etched inside. [4] A microscope image of the hole patterns is shown on the left in figure 1. The application of a voltage difference between the two metal sides of the foil produces concentrated dipole electric fields in the holes, accelerating and multiplying the electrons in their passage. The use of multiple GEM foils in a cascade setup allow for high gains without too high voltage differences on the single foil. A scheme of the detector structure can be seen on the right in figure 1.

The signal is formed at the charge collection anode, featuring two perpendicular sets of 256 strips, with a pitch of 400 μm and separated by polymer ridges of 50 μm. The different width of the X and Y strips is optimized to obtain equal charge sharing on the two axes for each event. A scheme of the strip structure is shown in figure 2. The active area of the detector is approximately 10×10 cm^2.

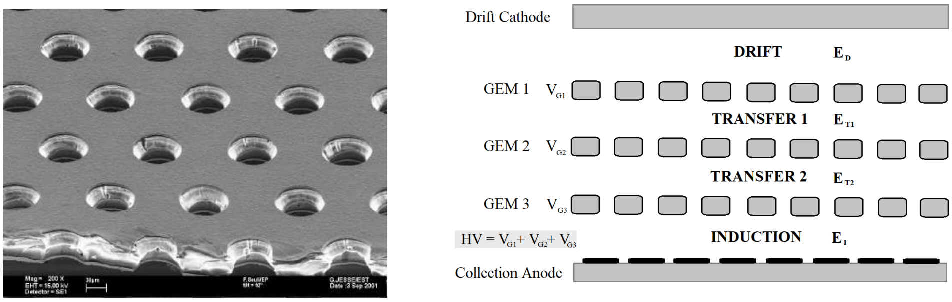

Figure 1. On the left, microscope image of the GEM foil hole pattern. On the right, schematics of the Triple-GEM detector.

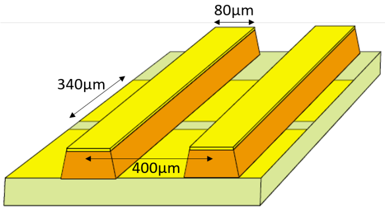

Figure 2. Schematics of the XY-strip structure of the anode.

The readout electronics is a fully digital chain composed of a combination of custom-made GEMINI ASICs [5] and FPGA boards, registering time of arrival, channel and time-over-threshold (ToT) for each event. The detector is a very fast and accurate single photon counter. Upon calibration, the information about ToT of each event can be translated in charge (and energy) of the incoming X-rays.

The application of a suitable converter, either deposited on the GEM foils [6] or in the active volume gas mixture [7], would allow for the detection of neutrons through the products of their conversion, with the same detector concept. The same system presented in this work will be modified to be employed for neutron imaging, following the same concept illustrated in [6].

3 Detector characterization

The optimal value for the detector parameters, namely the cumulative voltage difference across the foils (HV) and the threshold for each channel, have been found by analysis of the detector response in terms of counting rates. The HV parameter has been optimized to obtain full charge deposition of the incoming events (see [8] for details on the procedure), and the thresholds have been adjusted on the basis of the suppression of noise in the experimental environment. Charge calibration has been performed observing a single photo-emission peak (Ti fluorescence was used, with an energy of 4.5 keV), based on the variation of ToT values depending on the HV value applied, as described in [9].

Reconstruction of the single events is done through center-of-gravity method, with separate analyses of X and Y strips followed by event merging. This procedure imposes an operational limit on the high-rate capabilities of the detector, due to the production of artefacts in the image caused by the algorithm. Operation at high-rates has been studied with the use of stainless-steel masks. The detector was irradiated by X-rays, with covers on the window having different numbers of holes drilled at various locations. As an example, figure 3 shows the comparison of the image obtained at an average count rate on the detector of $6.81 \cdot 10^5$ Hz (on the left), where the two diagonal holes in the mask can be clearly seen with no other features in the 2D map, with respect to another image taken with the same mask at an average rate of $4.29 \cdot 10^6$ Hz (on the right). The software algorithm is not fully capable of reconstructing all events in the right places, and some X and Y events are wrongly matched, leading to the appearance of two additional holes in the opposite angles of the real ones. Additional dedicated studies will be focused on the algorithm to understand if it is possible to correct for these artefacts in some way.

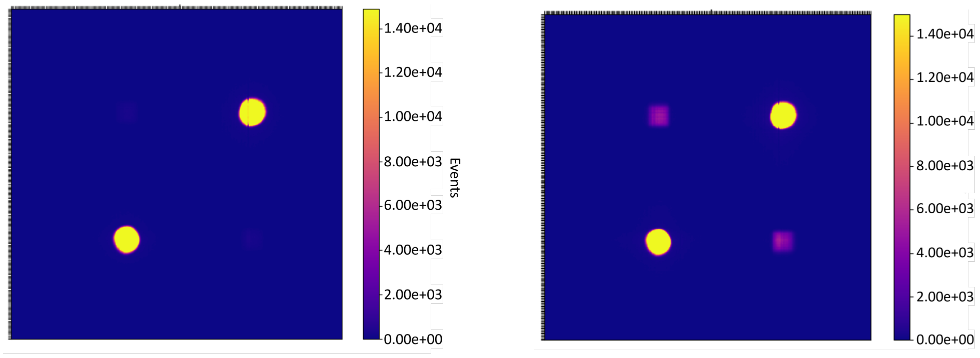

Figure 3. Example of production of artefacts in the reconstruction algorithm, with comparison of images taken at different rates ($6.81 \cdot 10^5$ Hz on the left, $4.29 \cdot 10^6$ Hz on the right).

4 Bone imaging

In order to demonstrate the capabilities of the new detector developed in this work, X-ray transmission imaging was performed on bone mock-ups. The experimental setup of the measurement can be seen in figure 4. The specimens were put in between the detector and the X-ray source. The X-ray tube was operated at a voltage of 10 kV and with a current of 5 µA. Irradiation lasted less than 10 seconds for each sample.

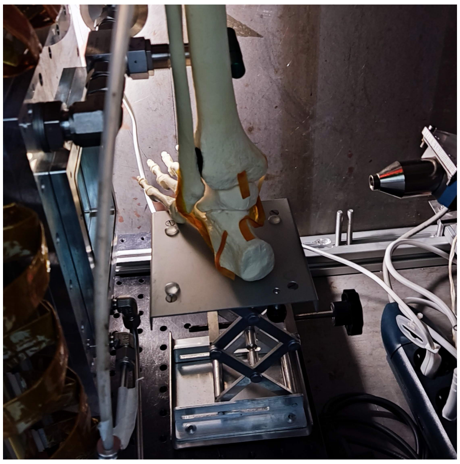

Figure 4. Experimental setup of the bone transmission measurements.

Different bone-like structures were observed. Figure 5 shows the resulting images, obtained by plotting directly the data coming from the detector, with a simple normalization to the empty beam image (i.e. the count rate obtained without samples in between the X-ray gun and the detector). The color scales of the images were adjusted to obtain a visually pleasing results and were not result of contrast optimization or other post-processing operation.

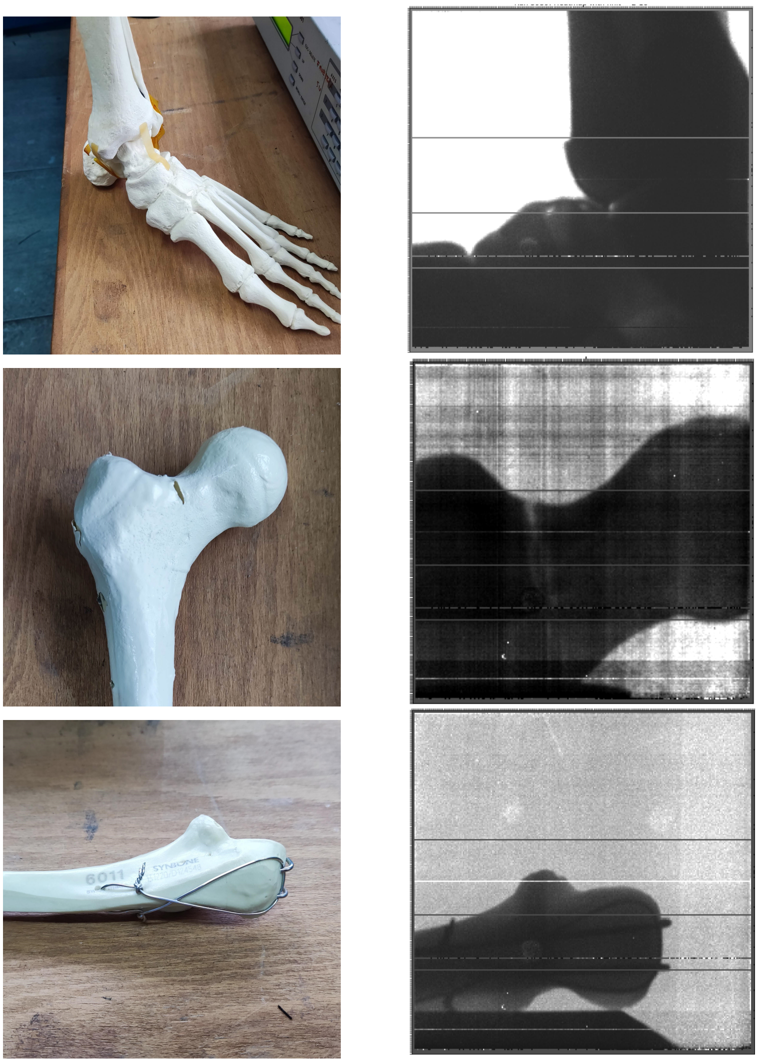

Figure 5. On the left, picture of the observed bone mock-ups. On the right, corresponding images captured with the detector.

The images show qualitatively the good spatial resolution that can be achieved with the use of the XY-strip anode structure, being able to distinguish structures smaller than a millimeter. It is to be noted that the measurement was only a preliminary observation: the parameters of the setup, namely voltage and current of the X-ray gun, as well as distance and position of the sample and the detector, can be subject to optimization to lead to better results. Additional dedicated studies will be also performed to quantify more accurately the spatial resolution obtainable.

5 Conclusions and perspectives

In this work, the development of a new GEM-based detector with a XY-strip anode pattern was presented. The properties of this kind of detector offer good perspectives for the analysis of different samples through X-ray and neutron imaging techniques. The characterization of the detector was presented, and a first demonstration of its capabilities was shown.

Future perspectives include the possibility of advanced studies on high-rate measurements and optimized imaging experiments. In addition, the upgrade of the system with the addition of a suitable converter, to be used for neutron imaging, is under way.

References

[1] N. Kardjilov, I. Manke, A. Hilger, M. Strobl and J. Banhart, *Neutron imaging in materials science*, *Mater. Today* **14** (2011) 248.

[2] D.D. Martino et al., *A neutron diffraction and imaging study of ancient iron tie rods*, 2018 *JINST* **13** C05009.

[3] M. Dinca and D. Mandescu, *Thermal neutron tomography for cultural heritage at inr*, *Phys. Procedia* **69** (2015) 646.

[4] F. Sauli, *The gas electron multiplier (GEM): Operating principles and applications*, *Nucl. Instrum. Meth. A* **805** (2016) 2.

[5] A. Pezzotta et al., *GEMINI, a CMOS 180 nm mixed-signal 16-channel ASIC for Triple-GEM detectors readout*, in the proceedings of the *IEEE SENSORS 2015*, Busan, Republic of Korea (2015), p. 1–4 [`DOI:10.1109/ICSENS.2015.7370468`].

[6] A. Muraro et al., *Mbgem: a stack of borated gem detector for high efficiency thermal neutron detection*, *Eur. Phys. J. Plus* **136** (2021) 1.

[7] S. Cancelli et al., *Characterisation of N2-GEM: a beam monitor based on Ar-N$_2$ gas mixture*, 2023 *JINST* **18** C05005.

[8] F. Caruggi et al., *Performance of a triple GEM detector equipped with Al-GEM foils for X-rays detection*, *Nucl. Instrum. Meth. A* **1047** (2023) 167855.

[9] A. Muraro et al., *Development and characterization of a new soft x-ray diagnostic concept for tokamaks*, 2019 *JINST* **14** C08012.